

The Influence of Graphitization on the Thermal Conductivity of Catalyst Layers and Temperature Gradients in Proton Exchange Membrane Fuel Cells

Robert Bock^{a,b}, Håvard Karoliussen^{a,2}, Bruno G. Pollet^{a,2}, Marc Secanell^{c,2}, Frode Seland^{b,2}, Dave Stanier^{c,2}, Odne S. Burheim^{a,1}

^aDepartment of Energy and Process Engineering, Norwegian University of Science and Technology, NO-7491 Trondheim, Norway

^bDepartment of Materials Science and Engineering, Norwegian University of Science and Technology, NO-7491 Trondheim, Norway

^cDepartment of Mechanical Engineering, University of Alberta, Edmonton, AB, Canada T6G 2R3

Abstract

As the proton exchange membrane fuel cell (PEMFC) has improved its performance and power density, the efficiency has remained unchanged. With around half the reaction enthalpy released as heat, thermal gradients grow. To improve the understanding of such gradients, PEMFC component thermal conductivity has been increasingly investigated over the last ten years, and the catalyst layer (CL) is one of the components where thermal conductivity values are still scarce. CLs in PEMFC are where the electrochemical reactions occur and most of the heat is released. The thermal conductivity in this region affects the heat distribution significantly within a PEMFC. Thermal conductivities for a graphitized and a non-graphitized CL were measured for compaction pressures in the range of 3 and 23 bar. The graphitized CL has a thermal conductivity of $0.12 \pm 0.05 \text{ WK}^{-1} \text{ m}^{-1}$, whilst the non-graphitized CL conductivity is $0.061 \pm 0.006 \text{ WK}^{-1} \text{ m}^{-1}$, both at 10 bar compaction pressure. These results suggest that the graphitization of the catalyst material causes a doubling of the thermal conductivity of the CL. This important finding bridges the very few existing studies. Additionally, a 2D thermal model was constructed to represent the impact of the results on the temperature distribution inside a fuel cell.

Keywords: Graphitization, CL, PEMFC, Thermal conductivity

1. Introduction

Renewable energy is the key to reducing anthropogenic green house gas emissions and climate changes. By means of hydrogen, produced renewably through water electrolysis, this energy can be stored and transported to when and where it is needed. [1] The stored chemical energy can then be converted back into electricity with the help of fuel cell technologies. This energy storage technology can be applied on a large scale to compensate for seasonal variations in renewable energy supply, but also on a smaller scale to compensate for mismatches in energy demand and supply on a daily basis [2]. A significant portion of the chemical energy fed to a PEMFC is converted into thermal energy

¹Corresponding author: burheim@ntnu.no

²Authors listed alphabetically

in addition to the desired electrical energy. Under normal operation, around 50% of the energy within a PEMFC is converted into heat [3]. The understanding and management of this heat is important when developing and optimizing PEMFC technology. Assessing the heat distribution in a PEMFC can help in shedding light on the governing kinetics and the water management within the cell [4]. Accurate thermal conductivity values of the subcomponents of the PEMFC are needed when predicting such temperature distributions with the help of modeling. In this work the focus is on catalyst layers. They can be produced with graphitized and non-graphitized carbon materials. The graphitization is thought to have an effect on the overall thermal conductivity of the catalyst layer, hence this study.

1.1. The catalyst layer

A PEMFC consists of a proton exchange membrane (PEM) with catalyst layers on both anode and cathode side, which are often applied directly onto the membrane to enhance ionic transport, thus creating a so-called catalyst coated membrane (CCM). Porous transport media are used to supply the reactant gases to the CLs and remove the product water on the cathode side. These are a mix of gas diffusion layer (GDL) made up of carbon fibers and microporous layer (MPL) created from carbon powder, both electrically conductive. The MPL is in direct contact with the CL and often created with PTFE to promote water removal even further [5]. These layers make up the membrane electrode assembly (MEA) which is compressed between conductive flow field plates that supply the reactant gases and collect the generated electrons.

The CLs foremost purpose is to facilitate the electrochemical reactions. It supplies active sites for the Platinum (Pt) particles that catalyze the reactions and it needs to provide pathways for moving electrons and ions as well as reactant gases. This is achieved by using a high surface area carbon support, that is electronically conductive, mixed with ionomer, that is ionically conductive, to create a porous material that satisfies the requirements for mass transport as well. [2]

The surface area of the carbon support providing the active sites for the Pt nanoparticles should be as large as possible for a good catalyzation of the reaction at high current densities [6].

1.2. Graphitization

The carbon material used in the creation of the catalyst layer has to be optimized for performance but also for longevity. Carbon material is prone to corrosion (oxidation) and during operation in a fuel cell as it is subjected to a corrosive environment with water present, potentials of more than +1 V, temperatures of around 80°C, and free oxygen. Corrosion decreases the available surface area over time, inhibiting the catalyzation of the electrochemical reaction [7]. The graphitization of the carbon beforehand mitigates the rate of corrosion of the catalyst support. A number of carbons are non-graphitizable, but for some a continuous and homogeneous development of the three-dimensional structure of graphite is observed upon heating the material beyond 1700°C [8]. This decreases the surface area by around one order of magnitude, but creates a rather corrosive-resistant support structure for the electrocatalyst. In addition, the electrical and thermal conductivities of the bulk material each increase by at least an order of

magnitude when graphitized. Stevens et al. (2005) reported that the stability of a BP2000 carbon catalyst support was significantly increased by graphitization at 3000°C at the cost of a dramatic reduction of surface area. The graphitized carbon catalyst support performed best compared to non-graphitized BP2000 and XC-72 carbon catalyst support materials in a fuel cell test over 75 hours. [6]

1.3. Thermal conductivity

The heat produced in a PEMFC originates mainly from the formation of water on the cathode catalyst layer near the middle of the membrane electrode assembly (MEA). In the adjacent layers, overpotentials and ohmic heating produce considerable heat as well [1]. As this heat is transported away from the middle of the MEA towards the cooling channels in the bipolar plates, temperature gradients arise. Their steepness depends on the thermal conductivities of the materials. Therefore, accurate thermal conductivity values are required to predict the temperature distribution in a fuel cell.

Khandelwal et al. (2006) experimentally measured and reported the through-plane thermal conductivity of dry Nafion®, various diffusion media, the catalyst layer, and the thermal contact resistance between diffusion media and a metal plate as a function of temperature and pressure experimentally. The thermal conductivity of a 0.5 mg cm⁻² platinum loaded catalyst layer was found to be $0.27 \pm 0.05 \text{ WK}^{-1}\text{m}^{-1}$. They estimated the maximum temperature drop for a 200 μm thick Sigracet GDL at 1.0 Acm⁻² to be 3-4 K with a one-dimensional analytical model. [9]

Burheim et al. (2010, 2014) started their work on thermal conductivity with wetted Nafion® membranes and SolviCore GDLs and continued to different catalyst layers both in dry and wet conditions [4, 10]. Their experimental methodology was applied to this work and is explained in detail. For the catalyst layers, they reported that the thermal conductivity of dry CLs and CLs with low water content was between 0.07–0.11 WK⁻¹m⁻¹ when 5-15 bar compaction pressure was used to compress the layers. When water was added, the thermal conductivity was influenced only when the water content was significantly higher than the capacity of the polymer. Thus the extra water, when the ionomer was oversaturated, caused the change in thermal conductivity found in the CL. The CLs tested were reported to compress almost irreversibly and to be incompressible beyond a compaction pressure of 10 bar. [10]

In another study, Burheim et al. (2014) investigated the thermal conductivity of lithium-ion battery electrode materials. A carbon cone based material was graphitized at 2700°C which increased the thermal conductivity from $0.07 \pm 0.01 \text{ WK}^{-1}\text{m}^{-1}$ before graphitization to $0.41 \pm 0.02 \text{ WK}^{-1}\text{m}^{-1}$ after heat treatment. [11]

Ahadi et al. (2017) recently published thermal conductivity values for a partially graphitized custom-made catalyst layer. They investigated the effect of hot-pressing, compression, measurement method, and substrate used on the through-plane thermal conductivity of the CL. The results were unaffected by these parameter variations and were reported to be $0.21 \pm 0.03 \text{ WK}^{-1}\text{m}^{-1}$ at 8 bar compaction pressure. [12]

To the authors' knowledge, at least four other research groups have studied and reported thermal resistances of fuel cell materials and contact resistance between the layers [13–18]. They investigated the influence of changes in

temperature, PTFE content, compaction pressure, and water content. Their findings are summarized in [19], however, none of these cover the thermal conductivity of the catalytic layer itself.

The challenge of handling the considerable heat production in future PEMFCs with increased effectiveness has been discussed in a recent review by Burheim and Pharoah [20]. While maximizing the power output and electrical efficiency of the PEMFC the produced heat inevitably increases beyond what is common today. Thus, knowing the temperature distribution in the PEMFC becomes even more important in the future. [20]

The present work aims to shed light on the surprisingly large effect of graphitization on thermal conductivity, and bridges the two existing studies on thermal conductivities of catalyst layers, one using amorphous carbon [10] and the other graphitized carbon [12]. The measured thermal conductivities in the two studies differ by a factor of three. The present work is an important bridge between the two existing studies of thermal conductivity of self standing CLs, as one was undertaken using amorphous carbon [10] and the other with graphitized carbon [12], with different manufacturing procedures. Observing the effect of graphitization may help explain why the two studies report results that differ by a factor of three.

1.4. Thermal models

To accurately predict the temperature distribution in new PEMFCs it is vital to understand the thermal behaviour of a PEMFC of different designs and under various operating conditions. Thermal modeling is very suitable for rapidly covering many different parameter variations, whereas experimental determination of the temperature distribution is invasive and has significant costs associated with it. Research interest on this topic started to surface around 20 years ago and has been gaining momentum ever since. Several research groups have published thermal models with varying degrees of detail [21–29], see [19] for a more detailed summary. In a recent book chapter, Secanell et al. (2017) review the current modeling approaches in PEMFCs, also discussing heat transport in detail [2]. Bhaiya et al. (2014) provided a very comprehensive thermal model that is available in the open-source code OpenFCST (openfcst.org) [30]. Zhou et al. (2018) recently coupled this thermal model with a two-phase flow model and analyzed the temperature distribution in a PEMFC with and without MPL [31]. Burheim and Pharoah (2017) pointed out the differences in modeled temperature distributions when taking all of the PEMFC layers into consideration [20]. They emphasize the future research needs on thermal gradients and heat aspects both experimentally and numerically.

In a separate review, Burheim (2017) discusses current knowledge about thermal conductivities in PEMFCs. He introduced a 2D thermal model of an MEA showing the effect of various parameters studied in existing literature. In the present work we employ a modified version of this model to investigate the temperature profile of the catalytic layer. [1]

2. Experimental

2.1. Thermal conductivity

The thermal conductivity measurements for this study were performed ex-situ in a custom-built measurement rig, a sketch of which is shown in Figure 1, similar to the one in [19]. This rig is designed to apply a constant heat flux through a cylindrical geometry that is symmetrical on top and bottom. This heat flux is induced by thermoelectric Peltier modules on either side, one heating, the other cooling. A pneumatic compression setup can apply up to 23 bar compaction pressure progressively throughout testing, so that samples and stacks of different thickness can be studied.

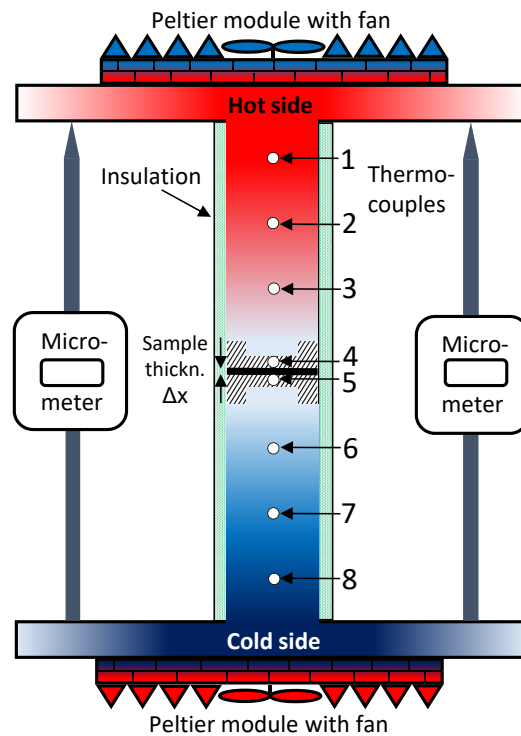


Figure 1: Sketch of the measurement rig

The thermal conductivity can be found from the relation between the heat flux and temperature gradient (Fourier's law). The one dimensional form of Fourier's law reads

$$q_x = -\kappa \frac{dT}{dx} \quad (1)$$

where q_x is the heat flux in the x-direction through the sample, κ is the thermal conductivity of interest and dT is the temperature change over the sample thickness dx . The heat flux is measured by six thermocouples, spaced equally apart both in the upper and the lower steel cylinders, to determine the heat flux through the rig and thus also samples. The temperature difference over the sample is measured by another two thermocouples that are situated inside an

aluminum cap on either side of the sample. Aluminum was chosen for its high thermal conductivity, which ensures a very close to uniform temperature distribution over the whole sample contact area. The thickness of the samples and how it may change is recorded by two Mitutoyo micrometers. A heat cap was designed and fitted around the steel cylinders to ensure the main heat transport in the longitudinal direction. With these values the thermal conductivity can be calculated with

$$\kappa = -q_x \frac{\Delta T}{\Delta x}. \quad (2)$$

The two catalyst layers measured here were custom-made and prepared in the laboratories of the University of Alberta for the very purpose of measuring their thermal conductivity. Sample NF1 contains 30wt% Nafion® and uses graphitized carbon (46wt% Pt/C Ketjen Black from TKK, max. 2.6 nm particle size [32]). Sample NF2 also contains 30wt% Nafion® but uses non-graphitized carbon (40wt% Pt/C Vulcan XC from Alfa Aesar, max. 4.5 nm particle size [Datasheet]). 20 layers of each ink were printed onto a copper foil ($\kappa_{copper} = 401 \text{ WK}^{-1}\text{m}^{-1}$, thickness = $19 \pm 3 \mu\text{m}$) with an inkjet printer (Dimatix DMP) resulting in a thickness of $10 \mu\text{m}$. The fabrication process is discussed in more detail in [33].

2.2. Modeling

The heat distribution inside a PEMFC was modeled with COMSOL Multiphysics using the model given in [1]. The impact of the performed thermal conductivity measurements was visualised with a 2D-model of the heat distribution. The model which does not include phase change for the produced water is used to indicate the importance of the different values for future models. Second order meshing was used which reduced the need for fine meshing and made for fast computing times, in the order of seconds. The main heat production occurs within the cathode catalyst layer due to the large overpotential (loss) for oxygen reduction. The excess heat must be transported away from the centre of the MEA through the layers to avoid overheating the membrane. Further heat sources consist of ohmic heating in the membrane and the anode catalyst layer. The geometry of the model is shown in Figure 2.

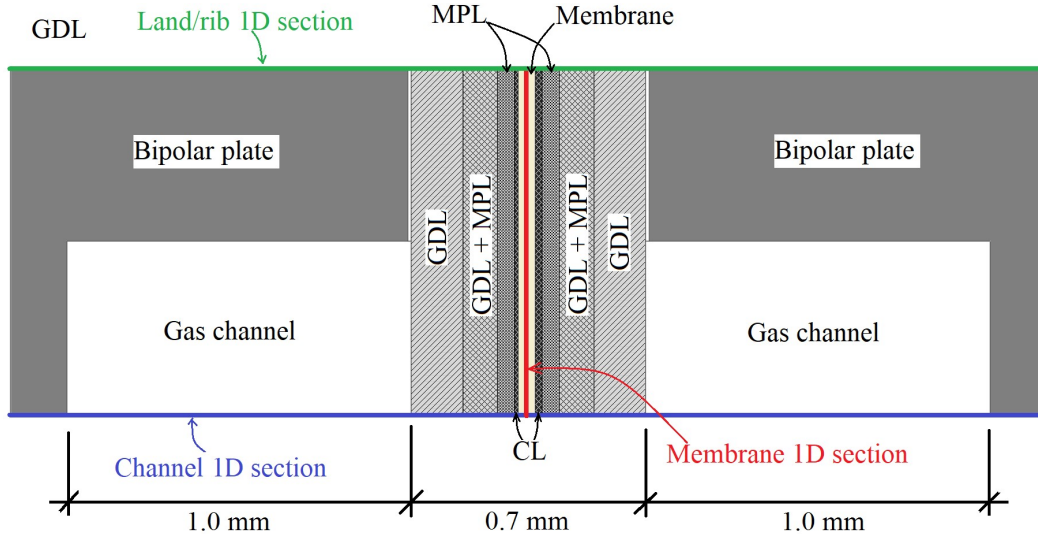


Figure 2: MEA geometry with coloured sections to show the base of the temperature distributions calculated in COMSOL, from Bock et al. [19]

The geometry includes part of a flow field channel and part of a flow field rib which is often also part of the bipolar plate (BP). This geometry is symmetrically cut from a larger fuel cell geometry and may thus be repeated to represent a larger cell. Thus, the boundaries where the cell could continue were modeled as adiabatic. The boundaries of the BPs on the very left and the very right in Figure 2 were modeled as isothermal, the temperature is modeled as constant here due to cooling channels in the BP outside of this control volume. See Burheim [1] for more details on the model being used. All the materials used in this work have individual thermal properties, which are summarized in Table 1).

Material	κ (through-plane)	κ (in-plane)	Thickness	ref.
	$\text{WK}^{-1}\text{m}^{-1}$	$\text{WK}^{-1}\text{m}^{-1}$	μm	
Bipolar plates	20	20		[34]
Air	0.024	0.024	1000	[35]
GDL, air-saturated	0.3	3	150	[19]
MPL-GDL integration	0.33	3.3	100	[19]
MPL	0.18	0.18	50	[36]
Anode CL NF1 graphitized	0.12	0.12	10	[*]
Anode CL NF2 non-graphitized	0.06	0.06	10	[*]
Cathode CL NF1 graphitized	0.12	0.12	20	[*]
Cathode CL NF2 non-graphitized	0.06	0.06	20	[*]
Membrane	0.25	0.25	50	[37]

Table 1: Thermal conductivities used in COMSOL model. In-plane κ values have been set to 10 times the value of through- plane κ in GDL and its composite.[15, 16] *values measured in this work at 10 bar compaction pressure.

The heat transfer in the gas channel is modeled by two different mechanisms. In the entire channel heat diffusion is applied. A $50\ \mu\text{m}$ boundary layer is defined at the bipolar plate walls and where the GDL limits the channel. Here, both heat convection and heat diffusion are applied. A $10\ \mu\text{m}$ thick air gap was implemented where the bipolar plate meets the GDL to account for thermal contact resistance (TCR).

Through-plane and in-plane thermal conductivities are known to differ significantly in GDL materials. According to measurements by Sadeghi et al. (2011) and Teertstra et al. (2011), in-plane thermal conductivities can be assumed ten times greater than through-plane thermal conductivities [15, 16]. The thermal conductivity values for GDLs found in Table 1 were taken at 10 bar compaction pressure. Due to the design of the flow field, the compaction pressure in the MEA varies from higher compaction pressure under the land/rib to lower compaction pressure in the gas channel. This variation in compaction pressure was assumed negligible for the model.

3. Results and Discussion

3.1. Thermal conductivity

The measured thermal conductivities are presented in Table 2. In addition, thermal conductivity values for two catalyst layers from literature are shown for comparison purposes.

Compaction pressure [bar]	NF1	NF2	NF1 to NF2	Non-Graphitized	Partially Graphitized
	Graphitized κ [$\text{WK}^{-1}\text{m}^{-1}$]	Non-Graphitized κ [$\text{WK}^{-1}\text{m}^{-1}$]	increase due to graphitization	20 wt% Pt/C [10] κ [$\text{WK}^{-1}\text{m}^{-1}$]	50 wt% Pt/C [12] κ [$\text{WK}^{-1}\text{m}^{-1}$]
3	0.10 ± 0.03	0.038 ± 0.008	161%		
5	0.11 ± 0.04	0.048 ± 0.005	129%	0.06 ± 0.03	0.20 ± 0.03
10	0.12 ± 0.05	0.061 ± 0.006	100%	0.07 ± 0.03	0.21 ± 0.03
15	0.14 ± 0.03	0.070 ± 0.018	103%	0.08 ± 0.03	0.22 ± 0.03
20	0.15 ± 0.05	0.10 ± 0.04	53%		
23	0.19 ± 0.11	0.114 ± 0.014	67%		

Table 2: Thermal conductivity values of different catalyst layers, values from [12] recalculated to match pressure

The results clearly show that the thermal conductivity is different for graphitized and non-graphitized carbon-based catalyst layers. The catalyst layer with graphitized carbon has a significantly higher thermal conductivity than the non-graphitized variant. Thermal conductivity is more than 50% higher for the highest compaction pressures, twice as high for 10 and 15 bar and more than twice as high for the lowest compaction pressure of 3 bar. This is also reflected in the literature values, where the non-graphitized carbon catalyst layer from [10] shows a thermal conductivity very close to the NF2 material and the partially graphitized material from [12] shows a significantly higher conductivity, even higher than for the NF1 material. All given materials show an increase in thermal conductivity towards higher compaction pressures.

The thermal conductivity results from Table 1 are visualized as a function of compaction pressure in Figure 3. Here, the originally measured values from [12] (Partially Graphitized) are shown.

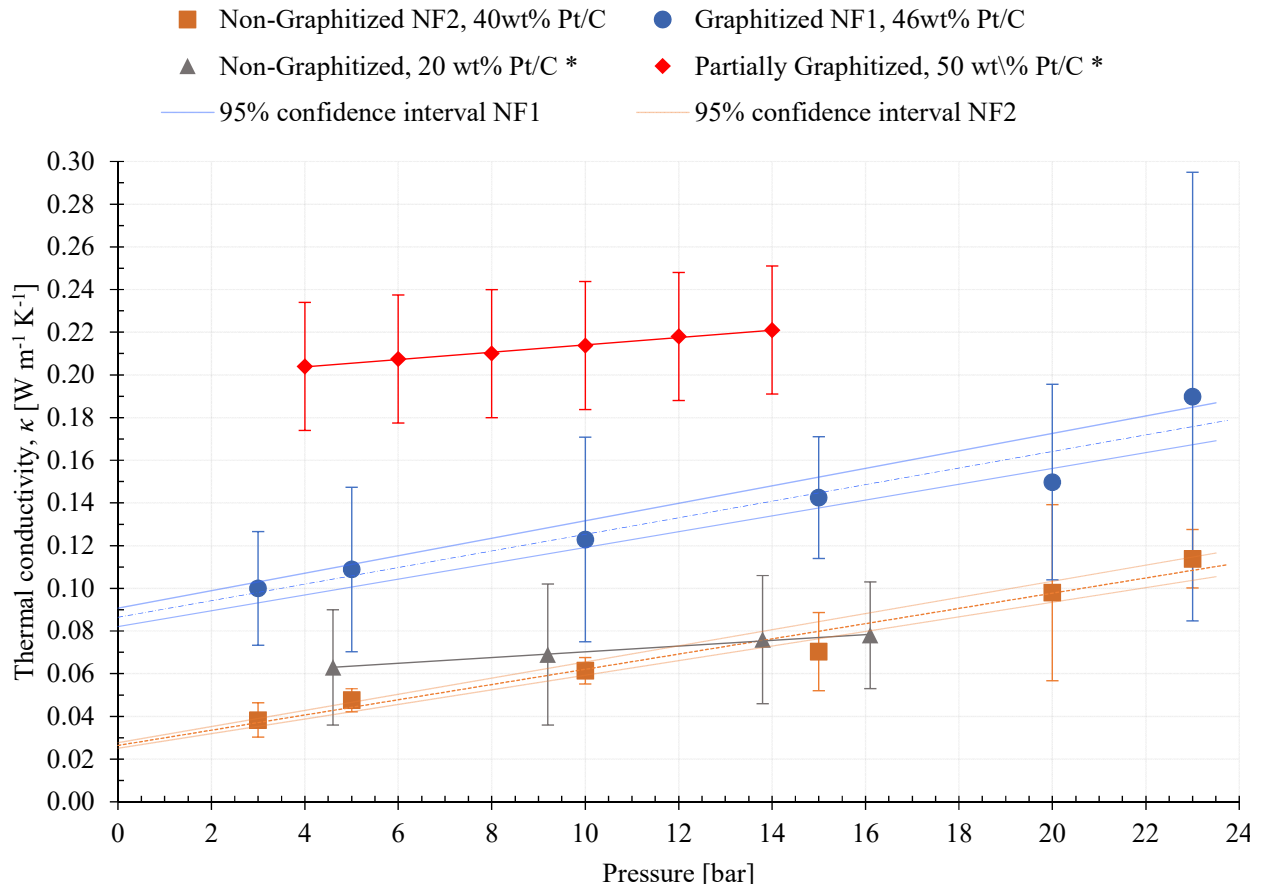


Figure 3: Thermal conductivity as a function of compaction pressure for graphitized and non-graphitized catalyst layers. *Literature values [10, 12]

NF1 and NF2 materials were compressed considerably, resulting in almost twice and more than twice the thermal conductivities of NF1 and NF2, respectively, for compaction pressures from 3 to 23 bar. The materials from [10] show less compressibility but the values agree very well with the NF2 material. Thermal conductivity values for partially graphitized CL from [12] are much higher than those obtained for NF1. The difference in thermal conductivity when comparing the graphitized material to available literature values from [12] may stem from the way the samples were produced. Our NF1 material was printed onto copper foil, where the material from [12] was bar coated onto aluminum foil. In addition, when the sample thickness is as low as $10\mu\text{m}$, measuring it poses a high uncertainty.

3.2. Modeling

The modeling results show a higher maximum temperature for the NF2 non-graphitized catalyst layer. It poses a higher thermal resistance to the heat removed from the fuel cell, resulting in a build-up of temperature. Figure 4 shows

the temperature distribution through the MEA where the bipolar plates are in contact with the GDL, as indicated by "Land/rib 1D section" in Figure 2. The dotted vertical lines visualize where different materials interface.

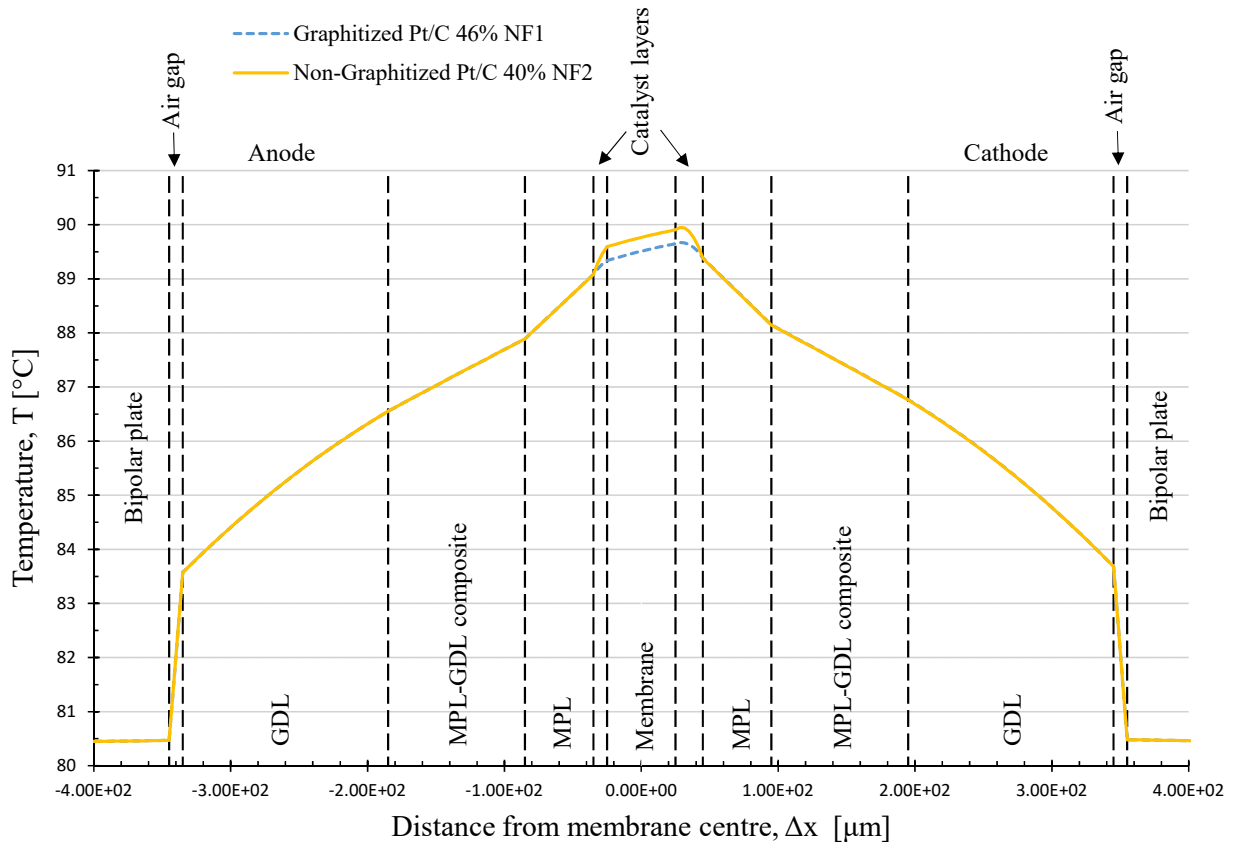


Figure 4: PEMFC land temperature profiles with graphitized catalyst layer vs. non-graphitized catalyst layer

The difference in temperature distribution when using NF1 or NF2 as catalyst layer in the model is limited to the membrane and the catalyst layers. As the heat is produced in the MEA only, the temperature profiles are equal outside of its three layers. Controlling the membrane temperature is crucial when designing a PEMFC. If the membrane overheats it may scorch and disable the whole fuel cell [38]. The observed difference in temperature in the membrane is ca. 1°C. The temperature is higher in the channel than under the land. The higher thermal conductivity of the bipolar plate causes better heat transport there than through the air in the channel resulting in a lower temperature under the land.

When modeling a system with residual water, the temperature gradient of the polarization plate, the GDL, and the MPL is lowered by a factor of more than three, yet the CL is likely to retain its temperature gradient; unless the CL is flooded, which in turn leads to a significantly lowered current density and thus lower temperature gradients. In this respect, the non-graphitized CL contributes to higher thermal gradients.

4. Conclusions

The thermal conductivity of CLs with either non-graphitized or graphitized carbon supports was measured. Results showed that graphitized CLs exhibit a higher thermal conductivity than non-graphitized CLs. The graphitized CL has a thermal conductivity of $0.12 \pm 0.05 \text{ WK}^{-1}\text{m}^{-1}$, whilst the non-graphitized CL conductivity is $0.061 \pm 0.006 \text{ WK}^{-1}\text{m}^{-1}$, both at 10 bar compaction pressure. This increase in thermal conductivity helps to explain the difference between the two existing studies of CL thermal conductivity.

When using graphitized carbon in a fuel cell model, the correct thermal conductivity value must be used to avoid producing misleading results of temperature and heat distribution. The heat distribution model used to analyze the impact of the change in thermal conductivity in this work showed clear temperature differences for graphitized and non-graphitized CLs. This suggests that an updated thermal conductivity value must be implemented where graphitized CLs are used in all future models and simulations regarding the temperature profile and transport of heat in the PEMFC to avoid introducing errors.

Acknowledgements

R. Bock thanks NTNU for providing him with a scholarship.

The cross-disciplinary ENERSENSE research framework is acknowledged for extra funding.

M. Secanell and D. Stanier thank the Natural Science and Engineering Research Council of Canada (NSERC) for its financial contribution.

References

- [1] O. Burheim, Review: PEMFC Materials' Thermal Conductivity and Influence on Internal Temperature Profiles, *ECS Transactions* 80 (2017) 509–525.
- [2] M. Secanell, A. Jarauta, A. Kosakian, M. Sabharwal, J. Zhou, *PEM Fuel Cells, Modeling*, Springer New York, New York, NY, 2017, pp. 1–61.
- [3] O. S. Burheim, *Engineering Energy Storage*, 1st ed., Elsevier Academic Press, 2017.
- [4] O. Burheim, P. Vie, J. Pharoah, S. Kjelstrup, Ex situ measurements of through-plane thermal conductivities in a polymer electrolyte fuel cell, *J. Power Sources* 195 (2010) 249–256.
- [5] Y. Chen, T. Tian, Z. Wan, F. Wu, J. Tan, M. Pan, Influence of ptfе on water transport in gas diffusion layer of polymer electrolyte membrane fuel cell, *Int. J. Electrochem. Sci* 13 (2017) 3827 – 3842.
- [6] D. A. Stevens, M. T. Hicks, G. M. Haugen, J. R. Dahn, Ex situ and in situ stability studies of pemfc catalysts: Effect of carbon type and humidification on degradation of the carbon, *Journal of The Electrochemical Society* 152 (2005) A2309–A2315.
- [7] J. D. Fairweather, D. Spornjak, A. Z. Weber, D. Harvey, SilviaWessel, D. S. Hussey, D. L. Jacobson, K. Artyushkova, R. Mukundan, R. L. Borupa, Effects of cathode corrosion on through-planewater transport in proton exchange membrane fuel cells, *J Electrochem Soc* 160 (2013) F980–F993.
- [8] R. E. Franklin, Homogeneous and heterogeneous graphitization of carbon, *Nature* 177 (1956) 239.
- [9] M. Khandelwal, M. Mench, Direct measurement of through-plane thermal conductivity and contact resistance in fuel cell materials, *J. Power Sources* 161 (2006) 1106–1115.
- [10] O. S. Burheim, H. Su, H. H. Hauge, S. Pasupathi, B. G. Pollet, Study of thermal conductivity of PEM fuel cell catalyst layers, *Int. J. Hydrogen Energy* 39 (2014) 9397–9408.
- [11] O. Burheim, M. Onsrud, J. Pharoah, F. Vullum-Bruer, P. Vie, Thermal conductivity, heat sources and temperature profiles of Li-ion batteries, *ECS Trans.* 58 (2014) 145–171.
- [12] M. Ahadi, M. Tam, M. S. Saha, J. Stumper, M. Bahrami, Thermal conductivity of catalyst layer of polymer electrolyte membrane fuel cells: Part 1 – experimental study, *Journal of Power Sources* 354 (2017) 207 – 214.
- [13] J. Ramousse, S. Didierjean, O. Lottin, D. Maillet, Estimation of the effective thermal conductivity of carbon felts used as pemfc gas diffusion layers, *Int. J. Therm. Sci.* 47 (2008) 1–6.
- [14] E. Sadeghi, N. Djilali, M. Bahrami, Effective thermal conductivity and thermal contact resistance of gas diffusion layers in proton exchange membrane fuel cells. part 2: Hysteresis effect under cyclic compressive load, *J. Power Sources* 195 (2010) 8104–8109.
- [15] E. Sadeghi, N. Djilali, M. Bahrami, A novel approach to determine the in-plane thermal conductivity of gas diffusion layers in proton exchange membrane fuel cells, *J. Power Sources* 196 (2011) 3565–3571.
- [16] P. Teertstra, G. Karimi, X. Li., Measurement of in-plane effective thermal conductivity in pem fuel cell diffusion media, *Electrochimica Acta* 56 (2011) 1670–1675.
- [17] N. Zamel, E. Litovsky, S. Shakhshir, X. Li, J. Kleiman, Measurement of in-plane thermal conductivity of carbon paper diffusion media in the temperature range of -20 °C to +120 °C, *Applied Energy* 88 (2011) 3042–3050.
- [18] N. Zamel, E. Litovsky, X. Li, J. Kleiman, Measurement of the through-plane thermal conductivity of carbon paper diffusion media for the temperature range from -50 to +120 °C, *Int. J. Hydrogen Energy* 36 (2011) 12618–12625.
- [19] R. Bock, A. D. Shum, X. Xiao, H. Karoliussen, F. Seland, I. V. Zenyuk, O. S. Burheim, Thermal conductivity and compaction of gdl-mpI interfacial composite material, *Journal of The Electrochemical Society* 165 (2018).
- [20] O. S. Burheim, J. G. Pharoah, A review of the curious case of heat transport in polymer electrolyte fuel cells and the need for more characterization, *Current opinion in electrochemistry* 5 (2017) 36–42.
- [21] T. V. Nguyen, R. E. White, A water and heat management model for proton-exchange-membrane fuel cells, *J. Electrochem. Soc.* 140 (1993).
- [22] M. Wöhr, K. Bolwin, W. Schnurnberger, M. Fischer, W. Neubrand, G. Eigenberger, Dynamic modelling and simulation of a polymer membrane fuel cell including mass transport limitation, *Int. J. Hydrogen Energy* 23 (1998).

- [23] A. Rowe, X. Li, Mathematical modeling of proton exchange membrane fuel cells, *Journal of Power Sources* 102 (2001).
- [24] N. Djilali, D. Lu, Influence of heat transfer on gas and water transport in fuel cells, *Int. J. Therm. Sci.* 41 (2002).
- [25] T. Berning, D. Lu, N. Djilali, Three-dimensional computational analysis of transport phenomena in a pem fuel cell, *Journal of Power Sources* 106 (2002).
- [26] H. Ju, H. Meng, C.-Y. Wang, A single-phase, non-isothermal model for pem fuel cells, *International Journal of Heat and Mass Transfer* 48 (2005).
- [27] U. Pasaogullari, C.-Y. Wang, Two-phase transport and the role of micro-porous layer in polymer electrolyte fuel cells, *Electrochimica Acta* 49 (2004).
- [28] C. J. Bapat, S. T. Thynell, Anisotropic heat conduction effects in proton-exchange membrane fuel cell, *Journal of Heat Transfer* 129 (2007).
- [29] S. G. Kandlikar, Z. Lu, Thermal management issues in a pemfc stack – a brief review of current status, *Applied Thermal Engineering* 29 (2009).
- [30] M. Bhaiya, A. Putz, M. Secanell, Analysis of non-isothermal effects on polymer electrolyte fuel cell electrode assemblies, *Electrochimica Acta* 147 (2014) 294–309.
- [31] J. Zhou, S. Shukla, A. Putz, M. Secanell, Analysis of the role of the microporous layer in improving polymer electrolyte fuel cell performance, *Electrochimica Acta* 268 (2018) 366–382.
- [32] J. C. Meier, C. Galeano, I. Katsounaros, J. Witte, H. J. Bongard, A. A. Topalov, C. Baldizzone, S. Mezzavilla, F. Schüth, , K. J. J. Mayrhofer, Design criteria for stable pt/c fuel cell catalysts, *Beilstein J Nanotechnol.* 5 (2014) 44–67.
- [33] S. Shukla, D. Stanier, M. S. Saha, J. Stumper, M. Secanell, Analysis of inkjet printed pefc electrodes with varying platinum loading, *J Electrochem Soc* 163 (2016) F677–F687.
- [34] R. Taherian, A review of composite and metallic bipolar plates in proton exchange membrane fuel cell: Materials, fabrication, and material selection, *Journal of Power Sources* 265 (2014).
- [35] J. Rumble (Ed.), *CRC Handbook of Chemistry and Physics*, 98 ed., Taylor & Francis, 2017.
- [36] O. S. Burheim, G. Ellila, J. D. Fairweather, A. Labouriau, S. Kjelstrup, J. G. Pharoah, Ageing and thermal conductivity of Porous Transport Layers used for PEM fuel cells, *J. Power Sources* 221 (2013) 356–365.
- [37] O. Burheim, P. J. S. Vie, S. Møller-Holst, J. Pharoah, S. Kjelstrup, A calorimetric analysis of a polymer electrolyte fuel cell and the production of H₂O₂ at the cathode, *Electrochim. Acta* 55 (2010) 935–942.
- [38] S. M. Summer, S. Nicholson, Abusive Testing of Proton Exchange Membrane Hydrogen Fuel Cells, Technical Report, U.S. Department of Transportation, Federal Aviation Administration, 2016.